

Understanding Complex Systems

Springer :
COMPLEXITY

Alexander Timokha *Editor*

Analytical and Approximate Methods for Complex Dynamical Systems

 Springer

Contents

General and Specific Problems of Complex Dynamical Systems	
Organising Centres in a 2D Discontinuous Map	3
Iryna Sushko, Viktor Avrutin, and Laura Gardini	
Phase Models for Coupled Oscillator Networks	29
Oleh Omel'chenko	
The Conflict Problem and Opinion Formation Models	47
Volodymyr Koshmanenko	
Dynamics of Conflict Interaction in Terms of Minimal Players	63
Oksana Satur	
Generalised Intermittency in Non-ideal and “Classical” Dynamical Systems	75
Aleksandr Shvets	
Lanchester’s Equations in Conflicting Sides Using ODEINT Python Library	89
Ihor Raynovskyy	
Reversible Saddle-Node Separatrix-Loop Bifurcation	101
Oleksandr Burylko, Matthias Wolfrum, and Serhiy Yanchuk	
Stationary and Travelling Synchronisation Patterns in Systems of Coupled Active Rotators	121
Oleh Omel'chenko and Matthias Wolfrum	
Continuum Media Modeling	
Complex Dynamical Systems of Two-Dimensional Sloshing in Rectangular Tank	137
Alexander Timokha	

Swirling-Type Sloshing in Square Base Tank Due to Orbital Excitations	171
Oleksandr Lagodzinskyi and Alexander Timokha	
Towards Kinetic Equations of Open Systems of Active Soft Matter	187
Viktor Gerasimenko	
Freely Oscillating Drop	205
Alexander Timokha	
Nonlinear WKB Method, Asymptotic Soliton-Like Solutions of Variable Coefficients Korteweg–de Vries Equations with Singular Perturbation and Rankine–Hugoniot-Type Conditions	225
Valerii Samoilenko, Yuliia Samoilenko, and Elvira Zappale	
Auxiliary Problems of Complex Dynamical Systems	
On Group Classification of Nonlinear Heat Equation: Algebraic Approach	259
Sofiia Huraka and Oleksandra Lokaziuk	
Mathematical Modelling of the Interconnected Boundary-Value Problems in the Hilbert Space	271
Oleksandr Pokutnyi	
Averaging in a Generalised Multifrequency System with a Delay	281
Yaroslav Bihun, Roman Petryshyn, and Ihor Skutar	
Exponentially Convergent Method for Hardy–Titchmarsh–Type Equation with Unbounded Operator Coefficient in Banach Space	295
Vitalii Vasylyk and Volodymyr Makarov	
Regularization of Linear Impulsive Boundary Value Problem for Systems of Integro-Differential Equations	319
Ivanna Bondar	
Interconnected System for the Lyapunov Equation with Control and Boundary Conditions	329
Oleg Iskra	
Lyapunov Function and Smooth Periodic Solutions to Quasilinear 1D Hyperbolic Systems	343
Irina Kmit and Viktor Tkachenko	
Author Index	377

Reversible Saddle-Node Separatrix-Loop Bifurcation



Oleksandr Burylko, Matthias Wolfrum, and Serhiy Yanchuk

Abstract We describe the unfolding of a special variant of the codimension-two Saddle-Node Separatrix-Loop (SNSL) bifurcation that occurs in systems with time-reversibility. While the classical SNSL bifurcation can be characterized as the collision of a saddle-node equilibrium with a limit cycle, the reversible variant (R-SNSL) is characterised by as the collision of a saddle-node equilibrium with a boundary separating a dissipative and a conservative region in phase space. Moreover, we present several reversible versions of the SNIC (Saddle-Node on Invariant Circle) bifurcation and discuss the role of an additional reversible saddle equilibrium in all these scenarios. As an example, we provide a detailed bifurcation scenario for a reversible system of two coupled phase rotators (a system on a 2D torus) involving a R-SNSL bifurcation.

Keywords Bifurcation · Time-reversibility · Coupled rotators · R-SNSL · Codimension-two · SNIC

O. Burylko (✉)

Institute of Mathematics of the National Academy of Sciences of Ukraine, Tereshchenkivska str. 3, 01024 Kyiv, Ukraine

e-mail: burylko@yahoo.co.uk

URL: <https://www.imath.kiev.ua/people/profile.php?pid=26&lang=en>

Institute of Mathematics, Humboldt University Berlin, Unter den Linden 6, 10099 Berlin, Germany

M. Wolfrum

Weierstrass Institute for Applied Analysis and Stochastics, Mohrenstrasse 39, 10117 Berlin, Germany

e-mail: wolfrum@wias-berlin.de

URL: <https://www.wias-berlin.de/people/wolfrum/>

S. Yanchuk

School of Mathematical Sciences, University College Cork, Western Road, Cork T12 XF62, Ireland

e-mail: syanchuk@ucc.ie

URL: <https://research.ucc.ie/profiles/D019/syanchuk@ucc.ie>

Potsdam Institute for Climate Impact Research (PIK), Potsdam 14437, Germany

© Springer Nature Switzerland AG 2025

A. Timokha (ed.), *Analytical and Approximate Methods for Complex Dynamical Systems*, Understanding Complex Systems, https://doi.org/10.1007/978-3-031-77378-5_7

1 Introduction

When modelling real-world processes using finite-dimensional dynamical systems, particularly ordinary differential equations, multiple parameters are inevitable. The choice of these parameters can significantly influence the system dynamics. Consequently, it is essential to examine how the properties of the dynamical system depend on these parameters. This has led to the development of the bifurcation theory [1, 11, 21, 26] and the discovery of various bifurcations such as Andronov-Hopf, saddle-node, transcritical, pitchfork, or homoclinic bifurcations. These bifurcations explain fundamental mechanisms of qualitative changes that can occur in the dynamics as the parameters are varied. They are classified as codimension-one bifurcations, which means they are “expected to occur when one parameter is varied” and they occur on codimension-one surfaces in the parameter space.

The codimension-two bifurcations occur on codimension-two surfaces in the parameter space, so they are not observed as “frequently” as the codimension-one bifurcations [8, 26]. At least two parameters should be adjusted to observe such points. However, it is now well established that codimension-two bifurcations play an essential role as organizing centres for the dynamics. For generic systems, all local (cusp, Bautin (or generalised Hopf), Bogdanov-Takens or fold-Hopf) and many of the global codimension-two bifurcations are well understood. In systems with an additional structure, such as (generalised) symmetry [17, 18, 32], or reversibility, the situation is completely different. Depending on the specific geometric configuration of the symmetry and the degenerate objects in phase space, the bifurcations come in many different versions implying different dynamical effects and having different unfoldings in parameter space.

The focus of this work is a reversible version of a classical codimension-two global bifurcation, the Saddle-Node Separatrix-Loop (SNSL) [10, 13, 40]. In the literature, the SNSL bifurcation is also known as the non-central saddle-node homoclinic point [2, 26]. The SNSL can be understood as the simultaneous occurrence of two codimension-one scenarios: a saddle-node bifurcation and a homoclinic loop that is connecting a stable and an unstable separatrix of the saddle-node. While the unfolding of the classical SNSL (see Fig. 4) is well known [10, 13, 40], we will present here a Reversible Saddle-Node Separatrix Loop (R-SNSL) bifurcation where the underlying dynamical system has additionally a specific time-reversal symmetry.

Reversibility is a feature that often occurs in real physical systems, and it also possesses some remarkable properties [5–7, 12, 20, 22, 29–31, 35, 37, 41, 43, 45, 49, 50, 52]. For example, such systems can have conservative-dissipative dynamics, where the phase space is divided into dissipative and conservative regions [7, 19, 37, 38, 47, 48].

Let us briefly recall the concept of reversible systems. We say that the system

$$\dot{x} = F(x), \quad x \in X, \tag{1}$$

has a time-reversal symmetry [28, 41] if there exists an involution \mathcal{R} of the phase space X satisfying

$$F(\mathcal{R}(x)) = -\mathcal{R}(F(x)) \quad (2)$$

and $\mathcal{R}^2 = \text{Id}$. In particular, time-reversibility implies that $\mathcal{R}(x(-t))$ is a solution of (1) if $x(t)$ is. The subspace

$$\mathbf{Fix}\mathcal{R} = \{x \in X : \mathcal{R}(x) = x\} \quad (3)$$

plays an important role in understanding the dynamics and phase space geometry of time-reversible systems. Note that, in contrast to the usual symmetry subspaces, $\mathbf{Fix}\mathcal{R}$ is not dynamically invariant for (1). Reversible systems have some properties that distinguish them from both dissipative and Hamiltonian systems.

- (i) For an equilibrium in $\mathbf{Fix}\mathcal{R}$, its stable and unstable manifolds are related by \mathcal{R} . Therefore, they have the same dimension. Also elliptic equilibria are possible.
- (ii) Equilibria outside $\mathbf{Fix}\mathcal{R}$ come in pairs related by \mathcal{R} and have opposite stability properties.
- (iii) There can be structurally stable homoclinic orbits limiting to equilibria in $\mathbf{Fix}\mathcal{R}$. Also structurally stable saddle-saddle connections between pairs of equilibria related by \mathcal{R} are possible.

The main results of the present paper can be briefly summarized as follows.

- We give the necessary conditions for two possible types of the R-SNSL bifurcation (see Fig. 2) and prove essential properties of their unfoldings.
- We show that the R-SNSL scenario must contain an additional saddle equilibrium located in $\mathbf{Fix}\mathcal{R}$.
- While the SNSL bifurcation can be roughly described as a collision of a limit cycle with a saddle-node equilibrium, the R-SNSL is characterised by the collision of a saddle-node equilibrium with the boundary between a dissipative and a conservative region in phase space.
- As an example, we describe in detail the unfolding of the R-SNSL bifurcation in a system of two coupled active rotators.

2 Reversible Saddle-Node Separatrix-Loop Bifurcation

The bifurcations we are going to investigate can all be described by a general reversible planar system

$$\frac{dx}{dt} = f(x, \mu), \quad x \in \mathbb{R}^2, \quad (4)$$

with smooth f and parameters $\mu = (\mu_1, \mu_2)$ from some open set $M \subset \mathbb{R}^2$ containing $(0, 0)$, which will be used to unfold the codimension-2 bifurcation points. We will

now give several assumptions that introduce the general geometric setting and specify the degeneracy assumptions introducing the bifurcations.

- (H1)** [Time-reversibility with one dimensional fixed space.] For all $\mu \in M$, there exists an involution \mathcal{R} with $f(\mathcal{R}(x)) = -\mathcal{R}(f(x))$ such that the fixed subspace

$$\mathbf{Fix}\mathcal{R} = \{x \in \mathbb{R}^2 : \mathcal{R}(x) = x\}$$

is one-dimensional. Without loss of generality, we may assume that

$$\mathcal{R} : (x_1, x_2) \longmapsto (x_1, -x_2) \quad (5)$$

for all $\mu \in \mathbb{R}^2$. In this case

$$\mathbf{Fix}\mathcal{R} = \{(x_1, x_2) : x_2 = 0\}. \quad (6)$$

- (H2)** [Existence of a saddle-node equilibrium.] There exists a one-dimensional family $\mu_{\text{sn}} \subset M$ with a nondegenerate saddle-node equilibrium $x_{\text{sn}} \notin \mathbf{Fix}\mathcal{R}$. Without loss of generality, we may assume this happens at $\mu_1 = 0$, i.e., $\mu_{\text{sn}} = (0, \mu_2)$ and that the Jacobian $Df(x_{\text{sn}})$ has the eigenvalues $\lambda_1 = 0$, $\lambda_2 < 0$. Moreover, we assume a generic unfolding of the saddle-node by μ_1 such that for $\mu_1 < 0$ there are two equilibria: a saddle \bar{x}_s with $\lambda_1 > 0$ and a node \bar{x}_n with $\lambda_1 < 0$, while there are no equilibria for $\mu_1 > 0$.
- (H3)** [Existence of a generic heteroclinic connection.] For all $\mu = (0, \mu_2) \in M$, the centre-unstable manifold $W^{cu}(x_{\text{sn}})$ of the saddle-node x_{sn} intersects $\mathbf{Fix}\mathcal{R}$.
- (H4)** [Existence of a non-generic heteroclinic connection.] For all $\mu \in M$, there is a reversible saddle equilibrium $x_s \in \mathbf{Fix}\mathcal{R}$. At $\mu = (0, 0)$, the intersection

$$W^{ss}(x_{\text{sn}}) \cap W^u(x_s) \quad (7)$$

is not empty. This global bifurcation is unfolded by the parameter μ_2 in the following way. For $\mu_1 = 0$ and $\mu_2 < 0$, the manifold $W^u(x_s)$ misses $W^{cs}(x_{\text{sn}})$ and follows along $W^{cu}(x_{\text{sn}})$. For $\mu_1 = 0$ and $\mu_2 > 0$, the manifold $W^u(x_s)$ lies inside $W^{cs}(x_{\text{sn}})$, i.e., it approaches x_{sn} along the centre-stable direction.

Note that the image $\mathcal{R}(x_{\text{sn}})$ is also a saddle-node equilibrium, but with second eigenvalue $\lambda_2 > 0$. Assumption (H3) implies the existence of a robust heteroclinic connection from x_{sn} to $\mathcal{R}(x_{\text{sn}})$. Assumption (H4) requires that the connection from $\mathcal{R}(x_{\text{sn}})$ back to x_{sn} is given as a structurally unstable heteroclinic chain that involves non-central connections with an intermediate reversible saddle equilibrium x_s .

The assumptions (H1)–(H4) for the reversible saddle-node separatrix-loop (R-NSNL) bifurcation are illustrated in Fig. 1. All together, they imply the existence of a reversible heteroclinic contour that contains three equilibria: the saddle-node x_{sn} , its image $\mathcal{R}(x_{\text{sn}})$, and an additional reversible saddle equilibrium x_s . This geometric setting can also be found in systems with a phase space of higher dimension. In this case,

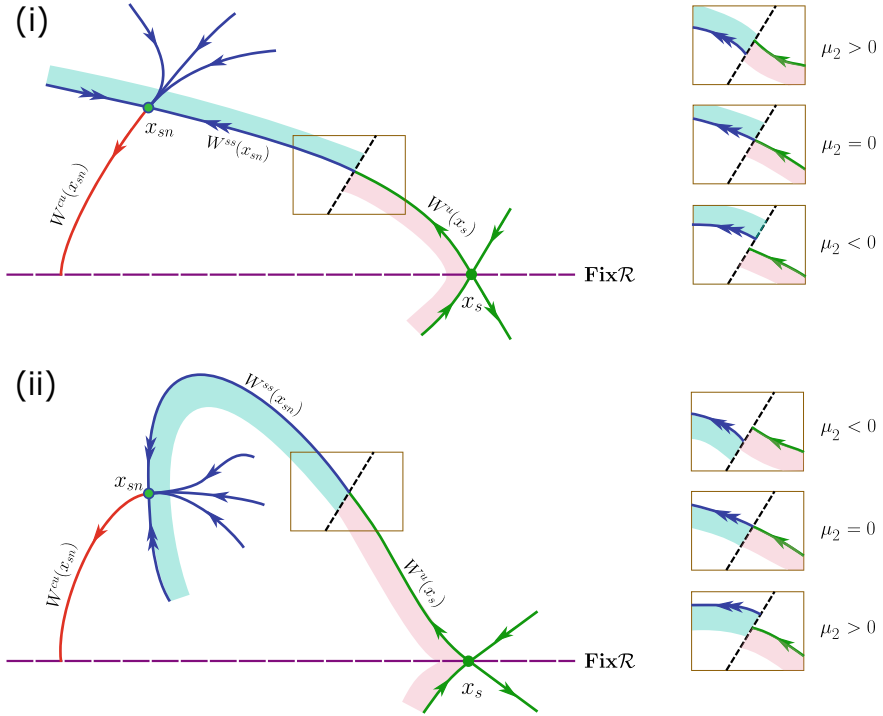


Fig. 1 Illustration of assumptions (H1)–(H4) for R-SNSL bifurcations. Fixed subspace \mathbf{FixR} according to (H1) (purple). Saddle-node equilibrium according to (H2) with centre-stable manifolds (blue). Generic intersection of its centre-unstable manifold (red) with \mathbf{FixR} according to (H3). Reversible saddle equilibrium with stable and unstable manifold (green). The non-generic heteroclinic connection (7) and its unfolding by μ_2 at a Poincaré section (dashed) according to (H4) is given in the boxes in the right row. The two different cases are distinguished by the fact that for $\mu = (0, 0)$ the reversible trajectories close to $W^u(x_s)$ (purple shaded region) can be outside (i) or inside (ii) of $W^{cs}(x_{sn})$ (blue shaded region)

the assumptions have to be reformulated with respect to a two-dimensional centre manifold, which should contain the two equilibria and have a one-dimensional intersection with \mathbf{FixR} . To avoid unnecessary technicalities, we restrict our presentation to the case of a two-dimensional phase space. Before we discuss the details of the two singular cases depicted in Figs. 1(i) and (ii) and the unfolding of this singularity, we first collect some general consequences related to assumptions (H1)–(H4).

Lemma 1 (Implications of reversibility (H1)) *Assume that system (4) has a break reversibility as specified in (H1). Then the following statements are true:*

1. All trajectories $x(t)$, $t \in \mathbb{R}$, satisfying (4), belong to one of the following classes:
 - (i) Trajectories where the orbit $\gamma = \{x(t) : t \in \mathbb{R}\}$ does not intersect \mathbf{FixR} .
 - (ii) Trajectories where the orbit has a single intersection with \mathbf{FixR} . They are called non-periodic reversible orbits. If, in addition,

$$\lim_{t \rightarrow \pm\infty} x(t) \in \mathbf{Fix}\mathcal{R},$$

we call the orbit a reversible homoclinic. If $x(t) \in \mathbf{Fix}\mathcal{R}$ for all $t \in \mathbb{R}$ the orbit is a reversible equilibrium.

- (iii) Trajectories where the orbit has exactly two intersections with $\mathbf{Fix}\mathcal{R}$. These are reversible periodic orbits.
2. Any point in $\mathbf{Fix}\mathcal{R}$ lying on a periodic orbit lies in an open intervals of such points in $\mathbf{Fix}\mathcal{R}$ and, hence, in a conservative region.
 3. The boundaries of the intervals with periodic points in $\mathbf{Fix}\mathcal{R}$ are given by reversible saddle equilibria or points on reversible non-periodic heteroclinic or homoclinic orbits.

Proof First, we show that any non-constant trajectory $x(t)$ with at least two intersections $x(t_1), x(t_2) \in \mathbf{Fix}\mathcal{R}$ and $t_1 < t_2$ is periodic and its orbit has exactly two intersections with $\mathbf{Fix}\mathcal{R}$. We can assume that for all t such that $t_1 < t < t_2$, we have $x(t) \notin \mathbf{Fix}\mathcal{R}$. Moreover, we can assume that, if there is the next intersection at some $t_3 > t_2$, then $|t_1 - t_2| \leq |t_2 - t_3|$. By reversibility, we can conclude from the assumption $x(t_2) = \mathcal{R}(x(t_2))$ that

$$x(t_1) = x(t_2 + t_1 - t_2) = \mathcal{R}(x(t_2 - t_1 + t_2)). \quad (8)$$

Here, we used that for any reversible trajectory with $x(0) \in \mathbf{Fix}\mathcal{R}$ we have $x(t) = \mathcal{R}(x(-t))$. Since by assumption also $x(t_1) \in \mathbf{Fix}\mathcal{R}$, it follows from (8) that $x(t_2 - t_1 + t_2) \in \mathbf{Fix}\mathcal{R}$. This implies that $t_3 = t_2 - t_1 + t_2$ and $x(t_1) = x(t_3)$, which proves that $x(t)$ is periodic and its orbit intersects $\mathbf{Fix}\mathcal{R}$ exactly twice.

Next, we show that an intersection of a non-constant trajectory $x(t)$ with $\mathbf{Fix}\mathcal{R}$ is always transversal. Indeed, at an intersection we have

$$f(x(t_1)) = f(\mathcal{R}(x(t_1))) = -\mathcal{R}(f(x(t_1)))$$

and it follows that the first component of $f(x(t_1))$, which is the component along $\mathbf{Fix}\mathcal{R}$, vanishes. Since $x(t)$ was assumed to be non-constant, the second component does not vanish. This proves transversality. From transversal intersection, we conclude that orbits with only one intersection are non-periodic. All other cases from statement (1) of the lemma are trivially satisfied.

Smoothness of the first-return map on $\mathbf{Fix}\mathcal{R}$ together with transversality implies the existence of open intervals with periodic points in $\mathbf{Fix}\mathcal{R}$ as stated in (2). At the boundary of these intervals, the return time has to become infinite. This implies that the trajectories through the boundary points are either reversible equilibria or lie on reversible non-periodic homoclinics or heteroclinics, as stated in (3).

Definition 1 (*SNIC in reversible systems (R-SNIC)*) Let x_{sn} be a saddle-node equilibrium as specified in (H1)–(H3). If also

$$W^{cs}(x_{\text{sn}}) \cap \mathbf{Fix}\mathcal{R} \neq \emptyset,$$

we call x_{sn} a *reversible saddle-node on invariant contour (R-SNIC)*.

Lemma 2 (R-SNIC touching a conservative region) *Let x_{sn} be an R-SNIC. If one of the branches of $W^{ss}(x_{\text{sn}})$ intersects $\mathbf{Fix}\mathcal{R}$, then any small neighborhood of it contains reversible periodic orbits. We say that x_{sn} is an R-SNIC that touches the corresponding conservative region.*

Proof The two branches of $W^{ss}(x_{\text{sn}})$ provide the boundary of $W^{cs}(x_{\text{sn}})$. If one of the branches of $W^{ss}(x_{\text{sn}})$ intersects $\mathbf{Fix}\mathcal{R}$, then close to the intersection point in $\mathbf{Fix}\mathcal{R}$ we find points that are not in $W^{cs}(x_{\text{sn}})$. Instead, their trajectories pass by x_{sn} , follow along $W^{cu}(x_{\text{sn}})$ and, due to (H3), intersect $\mathbf{Fix}\mathcal{R}$ a second time. According to Lemma 1 this implies that they are reversible periodic orbits, constituting a conservative region.

Theorem 1 (Two different types of R-SNSL) *Assume that (H1)–(H4) are satisfied. Then the R-SNSL bifurcation at $\mu = (0, 0)$ can be of two different types (see Figs. 1i and ii):*

- (i) *The family $\mu_{\text{sn}} = (0, \mu_2)$ of saddle-nodes x_{sn} changes at $\mu = (0, 0)$ from an R-SNIC that touches a conservative region ($\mu_2 > 0$) to a situation where this conservative region no longer touches x_{sn} . This happens if, close to the intersection $W^{ss}(x_{\text{sn}}) \cap W^u(x_s)$, there are no orbits in $W^{cs}(x_{\text{sn}})$ intersecting $\mathbf{Fix}\mathcal{R}$.*
- (ii) *The family $\mu_{\text{sn}} = (0, \mu_2)$ of saddle-nodes x_{sn} changes at $\mu = (0, 0)$ from an R-SNIC that touches a conservative region ($\mu_2 < 0$) to a situation where this conservative region has disappeared. This happens if all orbits in $W^{cs}(x_{\text{sn}})$ and close to the intersection $W^{ss}(x_{\text{sn}}) \cap W^u(x_s)$ intersect $\mathbf{Fix}\mathcal{R}$.*

Proof Assumptions (H1)–(H4) can be satisfied by two different configurations, which are shown in panels (i) and (ii) of Fig. 1. The two cases are distinguished by the fact that for $\mu = (0, 0)$ the reversible trajectories close to $W^u(x_s)$ (purple shaded region) can be outside (i) or inside (ii) of $W^{cs}(x_{\text{sn}})$ (blue shaded region). This implies that in the degenerate case at $\mu = (0, 0)$ close to the intersection $W^{ss}(x_{\text{sn}}) \cap W^u(x_s)$ in case (ii) there are orbits in $W^{cs}(x_{\text{sn}})$ (blue shaded region in Fig. 1) that also intersect $\mathbf{Fix}\mathcal{R}$ close to x_s (purple shaded region), while in case (i) there are no such orbits. However, in both cases this situation is degenerate and changes under small variations of μ_2 . According to (H4), the non-generic intersection $W^{ss}(x_{\text{sn}}) \cap W^u(x_s)$ is unfolded in a way such that for $\mu_2 > 0$ $W^u(x_s)$ intersects $W^{cs}(x_{\text{sn}})$. In case (i) this implies that for $\mu_2 > 0$ there are also nearby orbits in $W^{cs}(x_{\text{sn}})$ that intersect $\mathbf{Fix}\mathcal{R}$, and according to Lemma 2 we can conclude that x_{sn} is a R-SNIC that touches a corresponding conservative region. Additionally, for $\mu_2 > 0$, there emerges a new region of reversible heteroclinic connections from $\mathcal{R}(x_{\text{sn}})$ to x_{sn} . For $\mu_2 < 0$ the reversible orbits close to $W^u(x_s)$ (purple shaded region) still constitute a conservative region,

but x_{sn} lies no longer on the boundary of this region. This proves the assertions in part (i) of the theorem.

In case (ii), the situation occurs that there are orbits sufficiently close to $W^{ss}(x_{\text{sn}})$ that intersect $\mathbf{Fix}\mathcal{R}$ for $\mu_2 < 0$. Hence, we conclude that in this case an R-SNIC touches a corresponding conservative region. However, for μ_2 approaching zero from below, this conservative region becomes smaller and smaller, and it vanishes completely for $\mu_2 > 0$ (see Fig. 3(i)). This proves the assertions in part (ii) of the theorem.

Theorem 2 (Codimension-1 bifurcations in the unfolding of R-SNSL) *Assume that (H1)–(H4) are satisfied. Then in any neighborhood of $(\mu_1, \mu_2) = (0, 0)$ the following global codimension-one bifurcations can be found:*

- A heteroclinic saddle-saddle connection between x_s and \bar{x}_s .
- A heteroclinic orbit flip, where $W^u(x_s) \cap W^{ss}(\bar{x}_n) \neq \emptyset$.

Proof Consider first the situation for $\mu_1 = 0$. According to assumption (H4), for $\mu_2 < 0$ the manifold $W^u(x_s)$ misses $W^{ss}(x_{\text{sn}})$ and follows along $W^{cu}(x_{\text{sn}})$. For $\mu_1 = 0$ and $\mu_2 > 0$, the manifold $W^u(x_s)$ approaches x_{sn} along the centre-stable direction. This means that in a local Poincaré section, the intersection point of $W^u(x_s)$ is located on either side of the intersection point of $W^{ss}(x_{\text{sn}})$, depending on the sign of μ_2 (small panels in Fig. 1). According to (H2) for small $\mu_1 < 0$, x_s splits into the two equilibria \bar{x}_s and \bar{x}_n . Correspondingly, $W^{ss}(x_{\text{sn}})$ is split into $W^s(\bar{x}_s)$ and $W^{ss}(\bar{x}_n)$. This results into two intersection points with the local Poincaré section, which approach each other for $\mu_1 \rightarrow 0$. Hence, for fixed $\mu_2 \neq 0$ and sufficiently small $\mu_1 < 0$, the intersection point of $W^u(x_s)$ is located on either side of this pair of intersection points, depending on the sign of μ_2 . Keeping now $\mu_1 < 0$ fixed and varying μ_2 , the intersection point of $W^u(x_s)$ consecutively will coincide with either point of this pair. These intersections correspond to the two global codimension-one bifurcations in the statement of the theorem.

Theorem 3 (Conservative and dissipative regions at R-SNSL) *Assume that (H1)–(H4) are satisfied and $(\mu_1, \mu_2) = (0, 0)$. Then any neighborhood of x_{sn} contains dissipative and conservative regions.*

Proof The strong stable manifold $W^{ss}(x_{\text{sn}})$ of the saddle-node equilibrium divides a small neighborhood of x_{sn} in two parts. The centre-stable manifold $W^{cs}(x_{\text{sn}})$ is a dissipative region, since all trajectories in this neighborhood approach for $t \rightarrow \infty$ the saddle-node equilibrium. It remains to show that the other region contains a conservative part. To this end, we consider the intersection of $W^{cu}(x_{\text{sn}})$ with $\mathbf{Fix}\mathcal{R}$, which in (H3) is assumed to exist. As stated in the proof of Lemma 1, this intersection has to be transversal. According to the λ -Lemma (see [34]), a neighborhood of this point in $\mathbf{Fix}\mathcal{R}$ transported backward in time comes close to the strong stable manifold $W^{ss}(x_{\text{sn}})$. According to (H4), $W^{ss}(x_{\text{sn}})$ coincides with $W^u(x_s)$. Hence, in a small neighborhood of the intersection point we find trajectories that have a second intersection with $\mathbf{Fix}\mathcal{R}$ close to x_s . According to Lemma 1, this implies the existence of reversible periodic orbits and a conservative region. \square

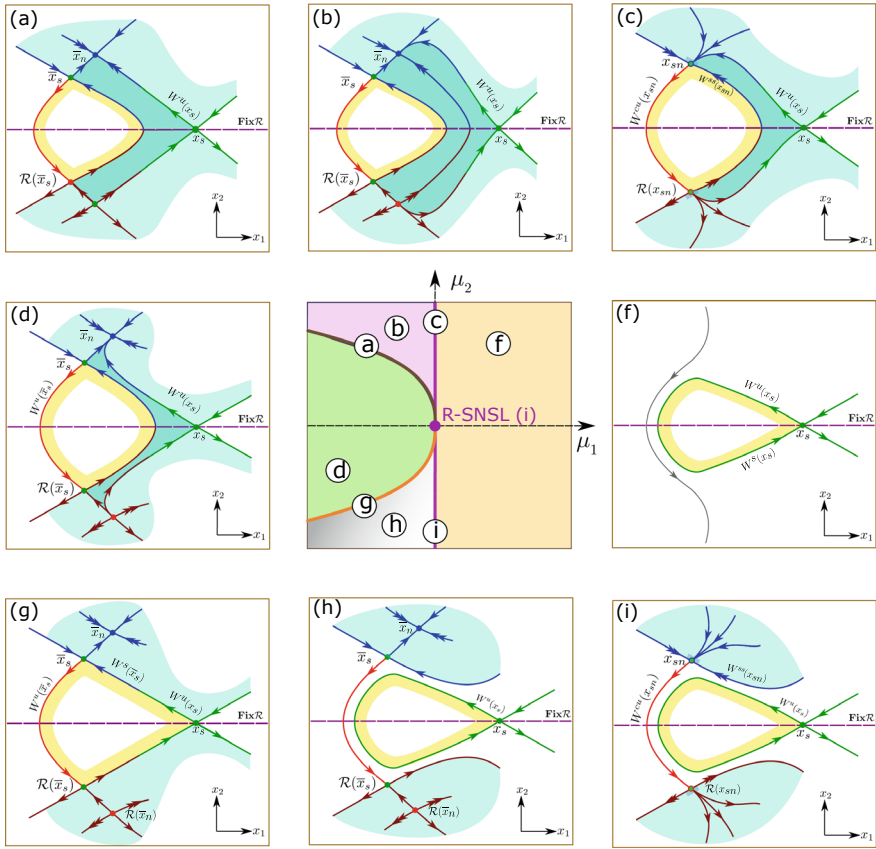


Fig. 2 Unfolding of the R-SNSL (i) bifurcation. The bifurcation diagram in the middle shows four different regions separated by codimension-one bifurcations. Saddle-node bifurcation (magenta); heteroclinic orbit flip (brown); heteroclinic saddle-saddle connection (orange). The corresponding schematic phase portraits are given in panels (a)–(i). Conservative region (yellow shading); dissipative region (blue shading); emerging dissipative region with reversible heteroclinics (darker shading)

In Figs. 2 and 3, we present the bifurcation diagram and the qualitatively different phase portraits in the unfolding of the two cases of the R-SNSL bifurcation. The bifurcation diagrams are identical and in both cases they contain a curve of saddle-node bifurcations and the two curves of global codimension-one bifurcations given in Theorem 2, which emanate from the codimension-two point. Each figure includes four structurally stable phase portraits (panels (b), (d), (f), (h)) and four phase portraits (panels (a), (c), (g), (i)) at different codimension-one bifurcations separating the structurally stable regions. Conservative and dissipative regions that intersect $\text{Fix}\mathcal{R}$ and are close to the reversible heteroclinic contour given in the assumptions are indicated by yellow and green shading.

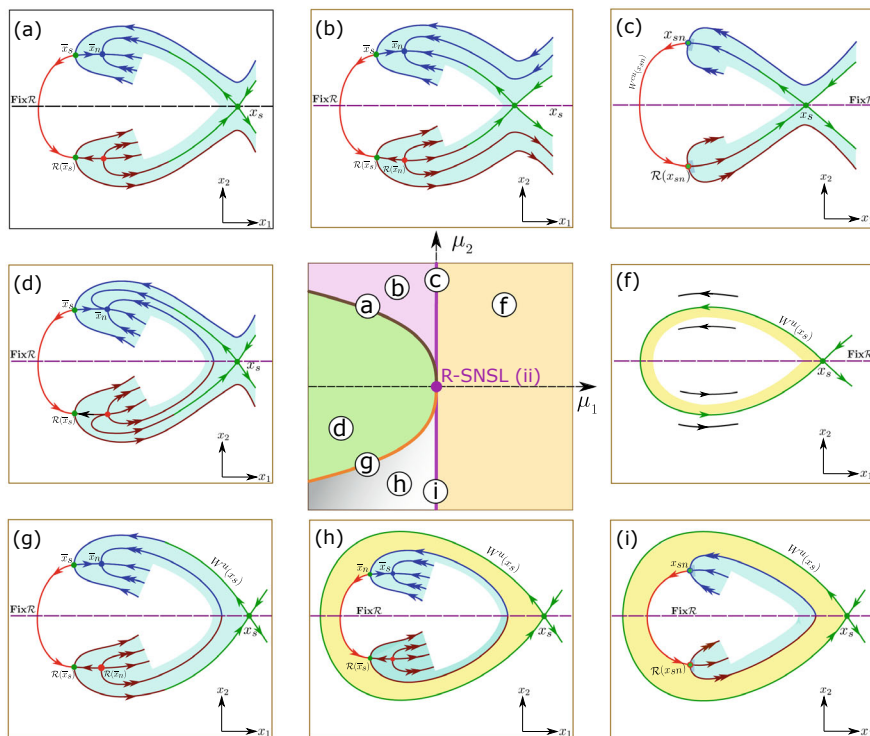


Fig. 3 Unfolding of the R-SNSL (ii) bifurcation. The bifurcation diagram in the middle shows four different regions separated by codimension-one bifurcations. Saddle-node bifurcation (magenta); heteroclinic orbit flip (brown); heteroclinic saddle-saddle connection (orange). The corresponding schematic phase portraits are given in panels (a)–(i). Conservative region (yellow shading); dissipative region (blue shading)

As stated in Theorem 3, in the degenerate case $\mu = (0, 0)$ there is both a conservative and a dissipative region close to the saddle-node equilibrium x_{sn} . Note that these regions behave differently in the two cases (i) and (ii). In case (i) there is a small reversible dissipative region that is present only for certain perturbations (a)–(d) and vanishes in the degenerate situation $\mu = (0, 0)$. In the case (ii) there is a small conservative region that is present only for certain perturbations (f), (h), (i) and vanishes for $\mu = (0, 0)$.

According to Theorem 1, both unfoldings include a R-SNIC that touches a conservative region shown in Figs. 2c and 3i. The unfolding of this singularity is given in Figs. 2b, c, f and 3h, i, f, respectively. Note that the phase portrait of the R-SNIC in Fig. 3c contains only a subset of orbits depicted in Fig. 2c. Indeed, in the case (ii), we cannot conclude from assumptions (H1)–(H4) whether the lower branch of $W^{ss}(x_{sn})$ actually intersects $\text{Fix}\mathcal{R}$. The assumption (7) refers here to the other branch of $W^{ss}(x_{sn})$.

The bifurcation diagram and the phase portraits in the unfolding show a great similarity to the classical SNSL bifurcation. Before we describe the similarities and differences to the reversible case in detail, we briefly recall some basic facts concerning this bifurcation. The saddle-node separatrix-loop bifurcation has been first described in [40] and later supplemented with more details in [10, 13]. It is characterized as a local saddle-node bifurcation in combination with a non-generic global reinjection entering along the non-central direction of the saddle-node equilibrium. This is, why it is often called *non-central saddle-node homoclinic* [2]. Its generic unfolding is sketched in Fig. 4. It is characterized by a curve of saddle-node bifurcations passing through the codimension-2 point and two curves of global bifurcations

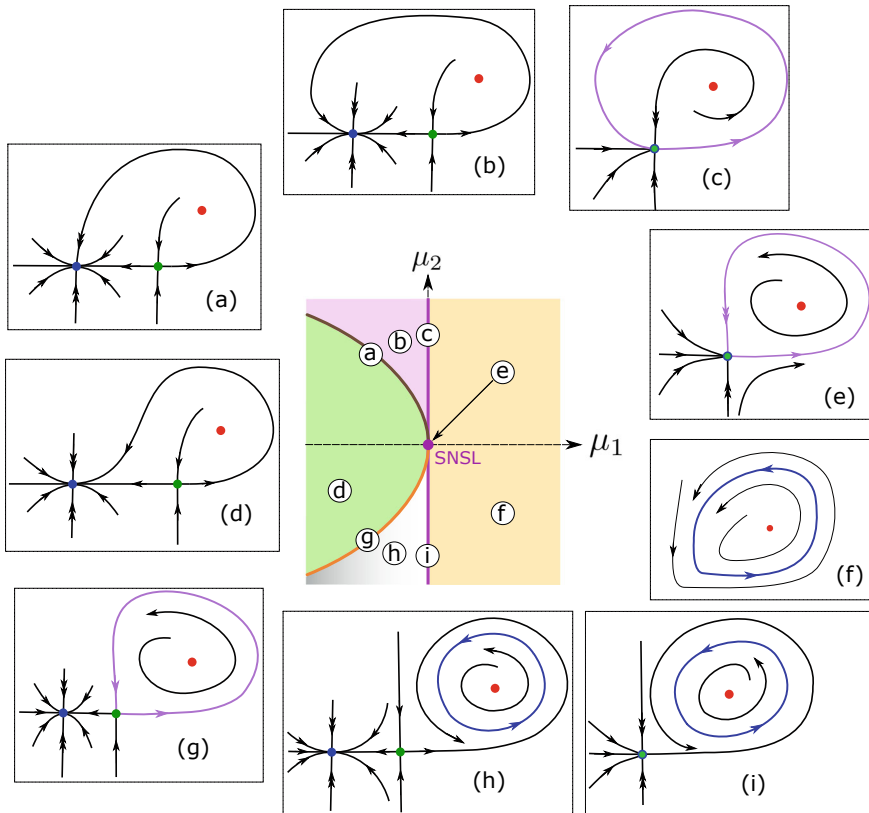


Fig. 4 Unfolding of the SNSL bifurcation. The bifurcation diagram in the middle shows four different regions separated by codimension-one bifurcations. The corresponding schematic phase portraits are given in panels (a)–(i). Magenta line and panels (c) and (i)—saddle-node bifurcation; brown curve and panel (a)—heteroclinic orbit flip; orange curve and panel (g)—generic homoclinic

emanating from this point. One of those is a usual homoclinic, i.e., the homoclinic to the saddle node equilibrium continues as a homoclinic to the saddle equilibrium that emerges in the saddle-node bifurcation. The other is a heteroclinic orbit flip, where the global reinjection along the non-central direction of the saddle-node equilibrium continues as a non-central heteroclinic connection, entering along the strong stable direction of the node. Roughly speaking, one can explain this bifurcation as a periodic orbit colliding with a saddle-node equilibrium. Another characterization is that along a curve of saddle-node bifurcations, this bifurcation marks up the transition from a SNIC to a usual non-SNIC saddle-node.

Both these characterizations apply also to the reversible case. There, reversible periodic orbits come in families, which constitute conservative regions. Hence, a collision of a saddle-node equilibrium can only occur with the boundary of a conservative region. Such a boundary typically consists of connecting orbits. In the simplest case, this can be a reversible homoclinic limiting to a reversible saddle equilibrium (cf. panel (f) in Figs. 2 and 3). This explains, why the additional equilibrium x_s is a necessary ingredient for the R-SNSL scenario.

Similar to the classical SNSL bifurcation, also the R-SNSL necessarily involves the reorganization of the global reinjection along a curve of saddle-node equilibria. While in the classical case this is just a transition from SNIC to non-SNIC, the situation in the reversible case is more involved. In a planar system with a reversibility as in (H1), the intersection

$$W^{cs}(x_{sn}) \cap \mathbf{Fix}\mathcal{R}$$

in general can consist of several open intervals, which can lead to arbitrarily complicated global configurations. In particular, a R-SNIC can lead to the emergence of several new conservative regions filled with reversible periodic orbits. We consider here only the reorganization at the edges of $W^{cs}(x_{sn})$, given by the two branches of $W^{ss}(x_{sn})$ and trajectories in their neighborhood.

An important result in [10, 13, 40] is the quadratic tangency at the SNSL point in parameter space of the two curves of global bifurcation to the saddle-node curve. It has been shown by Melnikov technique and reflects how the non-central manifold $W^{ss}(x_{sn})$ generically splits into the two non-central manifolds $W^{ss}(\bar{x}_n)$ and $W^s(\bar{x}_s)$ when the underlying saddle-node equilibrium x_{sn} splits into \bar{x}_n and \bar{x}_s . We believe that this result can be adapted in a straightforward manner to the reversible case presented here, but we refrained from elaborating the details in the present paper. Instead, we are going to underline the relevance of this bifurcation scenario by presenting an example of two coupled oscillators, where the R-SNSL bifurcation plays the role of an organizing centre for the dynamics.

3 The R-SNSL Bifurcation in a System of Two Coupled Active Rotators

Model and Its Symmetries

To illustrate the R-SNSL bifurcation and its unfolding, we consider the following system of two coupled active rotators. The rotators are counter-rotating and have an anti-reciprocal sinusoidal coupling:

$$\dot{\phi}_1 = \omega + \sin \phi_1 + \kappa \sin(\phi_1 - \phi_2), \quad (9)$$

$$\dot{\phi}_2 = -(\omega + \sin \phi_2) - \kappa \sin(\phi_2 - \phi_1), \quad (10)$$

where $\phi_1, \phi_2 \in \mathbb{T}^1 = \mathbb{R}/2\pi\mathbb{Z}$ are phase variables and the function $g(\phi) = \omega + a \sin(\phi)$ describes the local dynamics of the individual rotators, moving in opposite directions. For $|\omega| > 1$, both units are in an oscillatory mode (rotation) while for $|\omega| < 1$ they have a stable fixed point. The parameter κ gives the strength of the coupling. Note that the anti-reciprocal coupling can induce oscillations of the coupled system, where the individual oscillators do not perform full rotations, but oscillate around an equilibrium position (libration).

The active rotator model (sometimes called the nonuniform oscillator model [44]) plays an important role in electronics (phase-locked loops), mechanics, neuronal and biological systems [15], for the modelling of Josephson junctions, and other systems. Systems of coupled rotators can be found in the work by Shinomoto and Kuramoto [42] as well as in many later publications [3, 14, 16, 23–25, 27, 33, 36, 39, 46, 53, 54]. Reversible dynamics and bifurcations of a system of two coupled active rotators have been studied in detail in [6].

The system (9)–(10) has a time reversal symmetry given by the action

$$\mathcal{R} : (\phi_1, \phi_2, t) \mapsto (\phi_2, \phi_1, -t) \quad (11)$$

with the invariant subspace

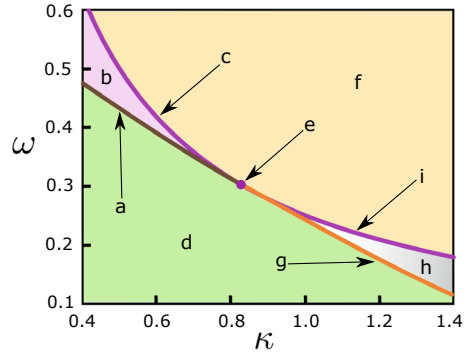
$$\mathbf{Fix}\mathcal{R} = \{(\phi_1, \phi_2) : \phi_1 = \phi_2\}. \quad (12)$$

The time reversibility of system (9)–(10) can be seen in the phase portraits of Fig. 6 as a reflection around the line $\phi_2 = \phi_1$ with the subsequent reversal of all arrows in opposite directions. In addition, system (9)–(10) possesses time-reversal *parametric* symmetries which are generated by the following actions

$$\gamma_\kappa : (\phi_1, \phi_2, \kappa, t) \mapsto (\pi - \phi_1, \pi - \phi_2, -\kappa, -t). \quad (13)$$

$$\gamma_\omega : (\phi_1, \phi_2, \omega, t) \mapsto (\phi_2, \phi_1, -\omega, -t), \quad (14)$$

Fig. 5 Bifurcation diagram for (9)–(10) in the parameter plane (κ, ω) in the neighborhood of the R-SNSL point (e). Bifurcation curves: magenta (c), (i)—saddle-node, orange (g)—saddle-saddle connection, brown (a)—homoclinic orbit flip



The presence of the symmetries (13) and (14) implies that the bifurcation diagram for (9)–(10) has mirror symmetries with respect to the parameters κ and ω .

The R-SNSL Bifurcation and Its Unfolding

This systems shows a R-SNSL point of type (i). The bifurcation diagram including the related codimension-one bifurcation lines for system (9)–(10) is shown in Fig. 5. The corresponding phase portraits are shown in Fig. 6.

The saddle-node bifurcation for the system (9)–(10) can be found analytically at

$$\omega = \frac{1}{4\kappa} \quad \text{for } |\kappa| > \frac{1}{2\sqrt{2}}. \quad (15)$$

These expressions can be obtained as follows. From the equilibrium condition of (9)–(10), one can derive

$$\sin(\phi_1 + \phi_2) = 4\omega\kappa \quad \text{for } \phi_1 \neq \phi_2,$$

which implies the necessary condition $4\omega\kappa = \pm 1$ for the saddle-node bifurcation. Furthermore, the solvability condition $\phi_1 \neq \phi_2$ implies that $|\kappa| > \frac{1}{2\sqrt{2}}$. This coincides with the fact that along the ellipse $4\kappa^2 + \omega^2 = 1$ a reversible pitchfork bifurcation [6, 51] takes place. At the codimension-two point of the intersection of these two bifurcation curves, which is not contained in Fig. 5, the curve of saddle-nodes meets **Fix** \mathcal{R} , is linked to its image under \mathcal{R} , and the corresponding curve in the parameter plane (κ, ω) ends.

The remaining two global bifurcation curves, the heteroclinic saddle-saddle connection (orange), and the heteroclinic orbit flip (brown) can be obtained only numerically. A suitable numerical method calculating an approximation for the connecting orbit by using projection boundary conditions is described in [4] and implemented in [9]. Typical phase portraits for parameters on these curves are shown in Fig. 6g and Fig. 6a, respectively.

All phase portraits in Fig. 6 contain conservative (yellow) regions bounded by homo/heteroclinic cycles and dissipative (white) regions. All of these conservative

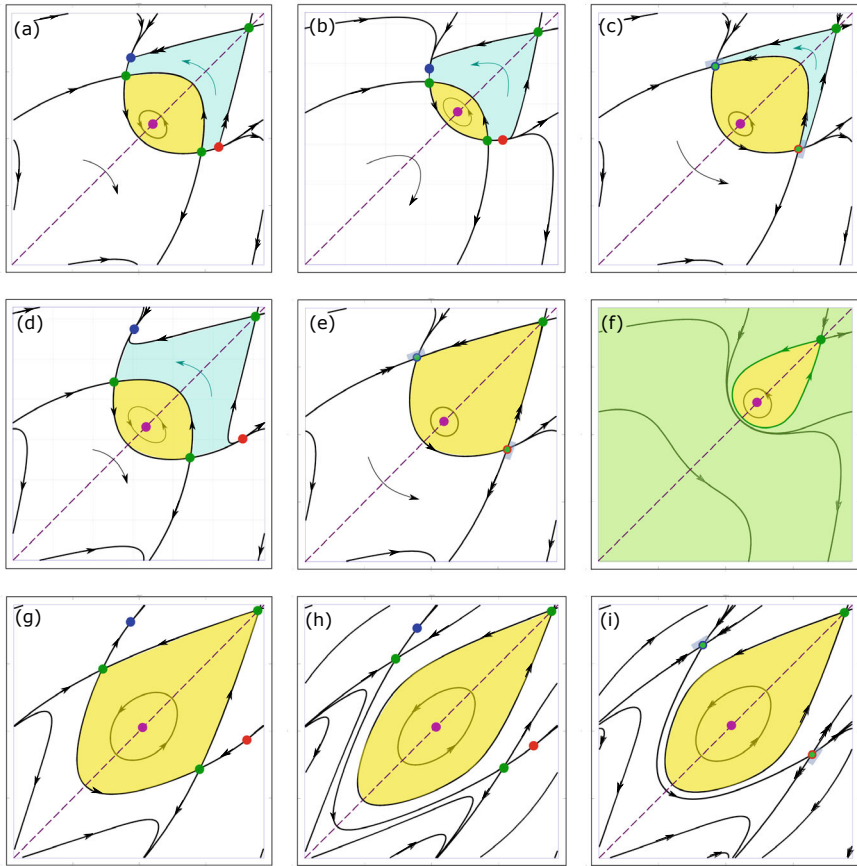


Fig. 6 Different types of phase portraits for (9)–(10) in the phase space $(\phi_1, \phi_2) \in [0, 2\pi] \times [0, 2\pi]$. Parameters from the correspondingly marked bifurcation curves and regions in Fig. 5. Structurally stable phase portraits—(b), (d), (f), (h). Codimension-one situations—(a), (c), (g), (i). Codimension-two R-SNSL point of type (i)—(e). Coloured regions: yellow—librations, green—rotations (conservative); white and blue—dissipative regions. Equilibrium points: red—source, blue—sink, green—saddle, magenta—centre. Degenerate equilibria are marked with two-coloured circles. The dashed purple line— $\text{Fix}\mathcal{R}$

regions have the simplest structure, i.e., each contains only a single centre-type equilibrium (as in Fig. 7a). Note that this is not part of our general assumptions (H1)–(H4), which refer only to the heteroclinic contour itself. Also a system of two coupled active rotators can have more complex conservative regions containing both dissipative and other conservative regions inside, in the case when the functions of the individual dynamics and the coupling function contain higher harmonics. Schematic pictures of several possible more complicated structures inside the heteroclinic contour are depicted in Fig. 7b, c.

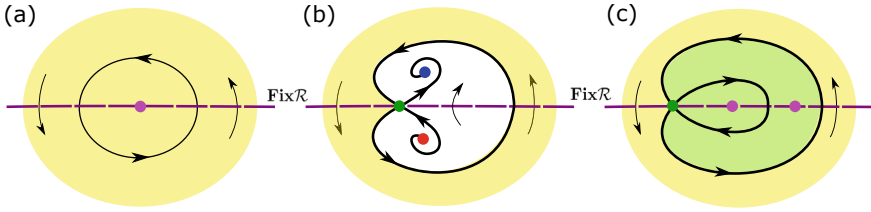


Fig. 7 Examples of schematic phase portraits of possible dynamics inside a conservative region. **a** A single conservative region with a single elliptic equilibrium. **b** A saddle equilibrium with a reversible homoclinic constitutes the boundary to a further dissipative region. **(c)** a saddle equilibrium with two reversible homoclinics constitutes the boundary to two further conservative regions. Stable, unstable and elliptic equilibria are marked by blue, red and magenta colours

4 Conclusions

With the R-SNSL (reversible saddle-node on separatrix-loop), we have described a codimension-two bifurcation point that can occur in reversible dynamical systems. This bifurcation is characterised by the simultaneous appearance of (i) a saddle-node away from the fixed subspace of the reversibility involution and (ii) a structurally unstable heteroclinic contour containing the saddle-node, its symmetric image under the involution transformation and their connections via the strong stable (unstable) manifolds to a saddle equilibrium within the fixed subspace. Such a codimension-two point is shown to describe the collision of a dissipative saddle-node equilibrium with a region of conservative dynamics. Thus, this scenario describes how the two basic components of reversible dynamics, dissipative and conservative, can interact.

The main elements in the unfolding of the R-SNSL conform to those in the unfolding of the classical codimension-two SNSL point: a codimension-one curve of saddle-nodes and two branches of global homoclinic or heteroclinic bifurcations. One of the most intriguing differences of the scenario we describe from the classical one is that it induces in two different scenarios the emergence of regions of phase space with conservative and dissipative dynamics, as well as regions foliated by heteroclinic orbits.

Our example of phase oscillators shows that the R-SNSL bifurcation can occur for coupled oscillator models where the coupling has the specific feature to be anti-reciprocal, i.e., the coupling terms have the same form but different signs for both oscillators. As shown in [6], also small generic perturbations, which break such a time reversal symmetry can induce interesting dynamical phenomena.

Acknowledgements The authors declare no conflict of interests. O.B. acknowledges hospitality at HU and the research group of Prof. B. Zwicknagl, as well as financial support by the National Research Foundation of Ukraine (Project 2020.02/0089) and the German Research Foundation (DFG), Project 195170736—SFB/TRR 109, Project 211504053—SFB 1060. S.Y. acknowledges the DFG Project 411803875. We also thank D. Turaev for useful discussions.

References

1. Arnold, V., Afrajmovich, V.S., Il'yashenko, Y., Shil'nikov, L.P.: Bifurcation Theory and Catastrophe Theory. Springer, Berlin (1999)
2. Bai, F., Champneys, A.R.: Numerical detection and continuation of saddle-node homoclinic bifurcations of codimension one and two. *Dyn. Stab. Syst.* **11**(4), 325–346 (1996). <https://doi.org/10.1080/02681119608806230>
3. Bačić, I., Yanchuk, S., Wolfrum, M., Franović, I.: Noise-induced switching in two adaptively coupled excitable systems. *Eur. Phys. J., Spec. Top.* **227**(10–11), 1077–1090 (2018). <https://doi.org/10.1140/epjst/e2018-800084-6>
4. Beyn, W.J.: The numerical computation of connecting orbits in dynamical systems. *IMA J. Num. Anal.* **10**(3), 379–405 (1990). <https://doi.org/10.1093/imanum/10.3.379>
5. Broer, H.W., Ciocci, M.C., Hanssmann, H.: The quasi-periodic reversible Hopf bifurcation. *Int. J. Bifurcat. Chaos* **17**(8), 2605–2623 (2007). <https://doi.org/10.1142/S021812740701866X>
6. Burylko, O., Wolfrum, M., Yanchuk, S., Kurths, J.: Time-reversible dynamics in a system of two coupled active rotators. *Proc. Royal Soc. A: Math., Phys. Eng. Sci.* 479 (2278) (2023). <https://doi.org/10.1098/rspa.2023.0401>
7. Burylko, O., Mielke, A., Wolfrum, M., Yanchuk, S.: Coexistence of Hamiltonian-like and dissipative dynamics in rings of coupled phase oscillators with skew-symmetric coupling. *SIAM J. Appl. Dyn. Syst.* **17**(3), 2076–2105 (2018). <https://doi.org/10.1137/17M1155685>
8. Champneys, A.R., Kuznetsov, Y.A.: Numerical detection and continuation of codimension-two homoclinic bifurcations. *Int. J. Bifurcat. Chaos* **4**(4), 785–822 (1994). <https://doi.org/10.1142/S0218127494000575>
9. Champneys, A.R., Kuznetsov, Y.A., Sandstede, B.: A numerical toolbox for homoclinic bifurcation analysis. *Int. J. Bifurcat. Chaos* **06**, 867–887 (1996). <https://doi.org/10.1142/S0218127496000485>
10. Chow, S.N., Lin, X.B.: Bifurcation of a homoclinic orbit with a saddle-node equilibrium. *Diff. Integral Eqn.* **3**(3), 435–466 (1990). <https://doi.org/10.57262/die/1371571144>
11. Crawford, J.D.: Introduction to bifurcation theory. *Rev. Mod. Phys.* **63**, 991–1037 (1991). <https://doi.org/10.1103/RevModPhys.63.991>
12. Delshams, A., Gonchenko, S., Gonchenko, V.S., Lázaro, J., Sten'kin, O.: Abundance of attracting, repelling and elliptic periodic orbits in two-dimensional reversible maps. *Nonlinearity* **26**(1), 1–33 (2013). <https://doi.org/10.1088/0951-7715/26/1/1>
13. Deng, B.: Homoclinic bifurcations with nonhyperbolic equilibria. *SIAM J. Math. Anal.* **21**(3), 693–720 (1990). <https://doi.org/10.1137/0521037>
14. Dolmatova, A., Goldobin, D., Pikovsky, A.: Synchronization of coupled active rotators by common noise. *Phys. Rev. E* **96**, 062,204 (2017). <https://doi.org/10.1103/PhysRevE.96.062204>
15. Ermentrout, G., Rinzel, J.: Beyond a pacemaker's entrainment limit: phase walk-through. *Am. J. Physiol.—Regulat. Integr. Comp. Physiol.* **246**(1), 102–106 (1984). <https://doi.org/10.1152/ajpregu.1984.246.1.R102>
16. Franović, I., Omel'chenko, O.E., Wolfrum, M.: Bumps, chimera states, and turing patterns in systems of coupled active rotators. *Phys. Rev. E* **104**, ID L052,201 (2021). <https://doi.org/10.1103/PhysRevE.104.L052201>
17. Golubitsky, M., Schaeffer, D.: Singularities and Groups in Bifurcation Theory. Volume I, Applied Mathematical Sciences, vol. 51. Springer, New-York (1985)
18. Golubitsky, M., Stewart, I.: The Symmetry Perspective. Birkhäuser Verlag, Basel (2002)
19. Golubitsky, M., Krupa, M., Lim, C.: Time-reversibility and particle sedimentation. *SIAM J. Appl. Math.* **51**(1), 49–72 (1991). <https://doi.org/10.1137/0151005>
20. Gonchenko, A., Gonchenko, S., Kazakov, A., Turaev, D.: On the phenomenon of mixed dynamics in Pikovsky-Topaj system of coupled rotators. *Physica D* **350**, 45–57 (2017). <https://doi.org/10.1016/j.physd.2017.02.002>
21. Guckenheimer, J., Holmes, P.: Nonlinear Oscillations, Dynamical Systems, and Bifurcations of Vector Fields. Springer (2002)

22. Homburg, A., Knobloch, J.: Multiple homoclinic orbits in conservative and reversible systems. *Trans. Am. Math. Soc.* **358**(4), 1715–1740 (2006). <https://doi.org/10.1090/S0002-9947-05-03793-1>
23. Ionita, F., Meyer-Ortmanns, H.: Physical aging of classical oscillators. *Phys. Rev. Lett.* **112**, ID 094,101 (2014). <https://doi.org/10.1103/PhysRevLett.112.094101>
24. Klinshov, V., Kirillov, S., Nekorkin, V., M. Wolfrum, M.: Noise-induced dynamical regimes in a system of globally coupled excitable units. *Chaos* **31**, ID 083,103 (2021). <https://doi.org/10.1063/5.0056504>
25. Kurrer, C., Schulten, K.: Noise-induced synchronous neuronal oscillations. *Phys. Rev. E* **51**, 6213–6218 (1995). <https://doi.org/10.1103/PhysRevE.51.6213>
26. Kuznetsov, Y.: *Elements of Applied Bifurcation Theory*. Applied Mathematical Sciences, vol. 112. Springer (1995)
27. Lafuerza, L., Colet, P., Toral, R.: Nonuniversal results induced by diversity distribution in coupled excitable systems. *Phys. Rev. Lett.* **105**, ID 084,101 (2010). <https://doi.org/10.1103/PhysRevLett.105.084101>
28. Lamb, J., Roberts, J.: Time-reversal symmetry in dynamical systems: a survey. *Physica D* **112**, 1–39 (1998). [https://doi.org/10.1016/S0167-2789\(97\)00199-1](https://doi.org/10.1016/S0167-2789(97)00199-1)
29. Lamb, J., Roberts, M.: Reversible equivariant linear systems. *J. Diff. Eqn.* **159**(1), 239–279 (1999). <https://doi.org/10.1006/jdeq.1999.3632>
30. Lerman, L., Turaev, D.: Breakdown of symmetry in reversible systems. *Regular Chaotic Dyn.* **17**(3), 318–336 (2012). <https://doi.org/10.1134/S1560354712030082>
31. Lim, C.C., McComb, I.H.: Time-reversible and equivariant pitchfork bifurcation. *Physica D: Nonlinear Phenomena* **112**(1), 117–121 (1998). [https://doi.org/10.1016/S0167-2789\(97\)00205-4](https://doi.org/10.1016/S0167-2789(97)00205-4)
32. Nijholt, E., Rink, B., Sanders, J.: Graph fibrations and symmetries of network dynamics. *J. Diff. Eqn.* **261**, 4861–4896 (2016). <https://doi.org/10.1016/j.jde.2016.07.013>
33. O’Keeffe, K., Strogatz, S.: Dynamics of a population of oscillatory and excitable elements. *Phys. Rev. E* **93**, ID 062,203 (2016). <https://doi.org/10.1103/PhysRevE.93.062203>
34. Palis, J., de Melo, W.: *Geometric Theory of Dynamical Systems: An Introduction*, 1st edn. Springer, New York (1982)
35. Parasyuk, I.O.: Conservation of quasiperiodic motions of reversible multifrequency systems. *Dokl. Akad. Nauk Ukrain. SSR A* **9**, 19–22 (1982). (in Russian)
36. Park, S., Kim, S.: Noise-induced phase transitions in globally coupled active rotators. *Phys. Rev. E* **53**, 3425–3430 (1996). <https://doi.org/10.1103/PhysRevE.53.3425>
37. Politi, A., Oppo, G.L., Badii, R.: Coexistence of conservative and dissipative behavior in reversible dynamical systems. *Phys. Rev. A* **33**, 4055–4060 (1986). <https://doi.org/10.1103/PhysRevA.33.4055>
38. Pikovsky, A., Rosenau, P.: Phase compactons. *Physica D* **218**(1), 56–69 (2006). <https://doi.org/10.1016/j.physd.2006.04.015>
39. Ronge, R., Zaks, M.A.: Emergence and stability of periodic two-cluster states for ensembles of excitable units. *Phys. Rev. E* **103**, ID 012,206 (2021). <https://doi.org/10.1103/PhysRevE.103.012206>
40. Schecter, S.: The saddle-node separatrix-loop bifurcation. *SIAM J. Math. Anal.* **18**(4), 1142–1156 (1987). <https://doi.org/10.1137/0518083>
41. Sevryuk, M.: *Reversible Systems*. Springer Lecture Notes in Mathematics. Springer, Berlin (1986)
42. Shinomoto, S., Kuramoto, Y.: Phase transitions in active rotator systems. *Progr. Theor. Phys.* **75**(5), 1105–1110 (1986). <https://doi.org/10.1143/PTP.75.1105>
43. Sprott, J., Hoover, W.G., Hoover, C.: Heat conduction, and the lack thereof, in time-reversible dynamical systems: generalized nosé–hoover oscillators with a temperature gradient. *Phys. Rev. E* **89**, ID 042,914 (2014). <https://doi.org/10.1103/PhysRevE.89.042914>
44. Strogatz, S.: *Nonlinear Dynamics and Chaos: with Applications to Physics, Chemistry, and Engineering*. Addison-Wesley, Biology (1994)

45. Teixeira, M.A.: Generic bifurcation of reversible vector fields on a 2-dimensional manifold. *Publicacions Matemàtiques* **41**, 297–316 (1997). <http://www.jstor.org/stable/43736585>
46. Tessone, C.J., Scirè, A., Toral, R., Colet, P.: Theory of collective firing induced by noise or diversity in excitable media. *Phys. Rev. E* **75**, 016,203 (2007). <https://doi.org/10.1103/PhysRevE.75.016203>.
47. Topaj, D., Pikovsky, A.: Reversibility vs. synchronization in oscillator lattices. *Physica D* **170**(2), 118–130 (2002). [https://doi.org/10.1016/S0167-2789\(02\)00536-5](https://doi.org/10.1016/S0167-2789(02)00536-5)
48. Tsang, K., Mirolo, R., Strogatz, S., Wiesenfeld, K.: Reversibility and noise sensitivity of josephson arrays. *Phys. Rev. Lett.* **66**, 1094–1097 (1991). <https://doi.org/10.1103/PhysRevLett.66.1094>
49. Vanderbauwhede, A.: Hopf bifurcation for equivariant conservative and time-reversible systems. *Proc. Royal Soc. Edinburgh, Sect.: Math.* **116**, 103–128 (1990). <https://doi.org/10.1017/S0308210500031401>
50. Wang, X., Xu, J., Zhang, D.: Degenerate lower dimensional tori in reversible systems. *J. Math. Anal. Appl.* **387**(2), 776–790 (2012). <https://doi.org/10.1016/j.jmaa.2011.09.030>
51. Wagenknecht, T.: About a homoclinic pitchfork bifurcation in reversible systems with additional \mathbb{Z}_2 -symmetry. *Nonlinearity* **15**, 2097–2119 (2002). <https://doi.org/10.1088/0951-7715/15/6/316>
52. Wagenknecht, T.: Two-heteroclinic orbits emerging in the reversible homoclinic pitchfork bifurcation. *Nonlinearity* **18**(2), 527 (2004). <https://doi.org/10.1088/0951-7715/18/2/004>
53. Zaks, M.A., Neiman, A.B., Feistel, S., Schimansky-Geier, L.: Noise-controlled oscillations and their bifurcations in coupled phase oscillators. *Phys. Rev. E* **68**, ID 066,206 (2003). <https://doi.org/10.1103/PhysRevE.68.066206>
54. Zaks, M.A., Tomov, P.: Onset of time dependence in ensembles of excitable elements with global repulsive coupling. *Phys. Rev. E* **93**, ID 020,201 (2016). <https://doi.org/10.1103/PhysRevE.93.020201>